ORIGINAL ARTICLE

Shoulder & Elbow

Shoulder & Elbow
2024, Vol. 0(0) 1–11

DOI: 10.1177/17585732241269193
journals.sagepub.com/home/sel


The association of rotator cuff muscle morphology and glenoid morphology in primary glenohumeral osteoarthritis

Deniz Siso[1], Hwabok Wee[1], Padmavathi Ponnuru[1], Gregory S Lewis[1], Jing Du[2], Gary F Updegrove[1], April D Armstrong[1] and Meghan E Vidt[3,4]

Abstract

Background: This retrospective study investigated associations of rotator cuff muscle atrophy (MA) and fatty infiltration (FI) with glenoid morphology.

Methods: Patients with primary glenohumeral osteoarthritis who presented to Penn State Bone and Joint Institute's orthopaedic clinic from September 2002 to December 2019 as total shoulder arthroplasty (TSA) candidates were evaluated. MA was determined by the cross-sectional area of each rotator cuff muscle on pre-operative MR and CT scans. Fat-free muscle and FI areas were quantified using Hounsfield units (HU). Glenoid morphology was assessed using glenoid version and inclination and modified Walch classification.

Results: Sixty-one patients (61 shoulders) were evaluated. B3 glenoids had a greater percent FI of supraspinatus (40.8 ± 7.3) versus A2 glenoids (31.6 ± 12.9, $p = 0.032$); infraspinatus and teres minor muscles (49.7 ± 9.1) versus A1 (31.1 ± 13.1, $p = 0.039$), A2 (30.2 ± 13.3, $p = 0.028$), and B1 glenoids (31.6 ± 11.9, $p = 0.038$); and subscapularis (36.7 ± 11.1) versus A2 glenoids (25.5 ± 14.7, $p = 0.032$). B2 glenoids had a larger area ratio of infraspinatus and teres minor to subscapularis (0.96 ± 0.16) than A1 (0.82 ± 0.13, $p = 0.026$) and A2 glenoids (0.57 ± 0.25, $p = 0.038$).

Conclusion: B3 glenoids had a greater FI of all rotator cuff muscles. B2 glenoids had a larger relative size of infraspinatus and teres minor muscles than subscapularis.

Keywords

rotator cuff muscle, fatty infiltration, muscle atrophy, glenoid morphology, glenohumeral osteoarthritis

Date received: 22nd December 2023; revised: 12th June 2024; accepted: 8th July 2024

Introduction

Muscle atrophy (MA) and fatty infiltration (FI) are two degenerative processes that can affect the rotator cuff muscle morphology.[1] Glenohumeral joint stability is provided by rotator cuff muscle force couples across the joint,[2,3] and any force imbalance of the joint can cause shoulder instability.[4,5] Rotator cuff MA and FI could alter the natural magnitude and distribution of muscle force across the joint, with adverse consequences on joint loading and stability. Previous work suggests that MA and FI could contribute to poor outcomes after total shoulder arthroplasty (TSA).[6,7]

Changes in glenoid morphology, such as eccentric glenoid wear, glenoid retroversion, and glenoid inclination, are common in primary glenohumeral osteoarthritis.[8,9] These changes in glenoid morphology also correlate with poor TSA outcomes.[10,11] Given the potential prognostic role of rotator cuff FI, MA, and glenoid morphology in clinical outcomes of TSA, it is clinically relevant to study these factors in association with each other to understand whether these processes are associated or independent factors that drive the TSA outcomes. Furthermore, research on muscle morphology could help drive the development of

[1]Orthopaedics and Rehabilitation, Penn State College of Medicine, Hershey, PA, USA
[2]Mechanical Engineering, Penn State University, University Park, PA, USA
[3]Biomedical Engineering, Penn State University, University Park, PA, USA
[4]Physical Medicine and Rehabilitation, Penn State College of Medicine, Hershey, PA, USA

Corresponding author:
Meghan E Vidt, 331 Chemical and Biomedical Engineering Building, Penn State University, University Park, PA 16802, USA.
Email: mzv130@psu.edu

interventions, such as prehabilitation, that target MA and FI to improve TSA outcomes. Studies that have investigated the association of MA and FI with glenoid morphology are few and have reported conflicting results.[12–16] Among the studies that have analyzed FI, Donohue et al.[12] (2018) reported a link between high-grade rotator cuff muscle FI and Walch type B3 glenoids. In contrast, Moverman et al.[13] (2022) recently did not demonstrate any association between rotator cuff muscle FI and Walch glenoid types. Aleem et al.[14] (2019) quantified MA and reported larger relative size of the posterior rotator cuff (infraspinatus and teres minor) muscle compared to the anterior rotator cuff muscle (subscapularis) in Walch B2 glenoids, while Moverman et al.[13] (2022) demonstrated larger absolute infraspinatus and teres minor muscle size in Walch type B glenoids. Thus, the role of MA and FI in the development of glenoid wear seen in primary glenohumeral osteoarthritis is unclear.

There are several challenges in assessing MA and FI and their association with glenoid morphology. First, the current standard method for measurements of FI is the semi-quantitative Goutallier classification system, which is limited by its high inter- and intra-observer variability.[17–19] Second, while the muscle area and volume have been studied in its association with glenoid morphology,[13–16] efforts have not been made to quantify the fat-free muscle area, which is the amount of muscle tissue within the segmented muscle boundary. We suspect that the fat-free muscle could play a role in the development of glenoid wear since it is the force-producing component of the rotator cuff muscles that dictates the force distribution and magnitude across the joint. Third, magnetic resonance imaging (MRI) is the current 'gold standard' imaging modality to assess skeletal muscle size.[17,20,21] However, compared to MRI, computed tomography (CT) scans are less expensive, provide a better visualization of the bone structures, and are more frequently obtained for surgical planning prior to TSA.[17] Thus, obtaining accurate MA and FI measurements from CT scans in clinical settings could save time and money, with recent evidence showing nearly equivalent measures can be obtained from MRI and CT.[17]

The primary purpose of the study was to determine the associations of rotator cuff MA and FI with glenoid morphology in primary glenohumeral osteoarthritis by quantifying the areas of the muscle, FI, and fat-free muscle. In addition, we assessed the use of CT for measures of muscle size via comparison with MRI.

Materials and methods

This was a retrospective study, approved by the Institutional Review Board at the Penn State College of Medicine. A total of 66 patients with primary glenohumeral osteoarthritis who presented to the orthopedic clinic from September 2002 to December 2019 as candidates for total shoulder arthroplasty and had pre-operative CT scans were evaluated.

Validation of CT scans for measures of muscle size

Following the methods described by Lehtinen et al.[20] (2003), the cross-sectional area of each rotator cuff muscle was segmented, which is a reliable and reproducible way to measure muscle size from MRI scans. Chalmers et al.[17] (2018) have recently shown that this method provides nearly equivalent measurements between either MRI or CT scans. To characterize the accuracy of CT scans for our measure of the muscle size, all patients who had both pre-operative MRI and CT scans were identified. Supraspinatus, infraspinatus and teres minor combined, and subscapularis muscles were segmented on each of the MRI and CT scans using Avizo software (Thermo Fisher Scientific, Inc., Waltham, WA) using the methods of Chalmers et al.[17] (2018) and manual segmentation techniques used in previous work.[22–24] Briefly, the scapula from MRI and CT was segmented on 2-dimensional (2D) slices to obtain three-dimensional (3D) images of the scapula, as shown in Figure 1(a) and (b). The 3D image of the scapula obtained from the CT segmentation was then re-oriented to superimpose it with the 3D image obtained from the MRI segmentation, as shown in Figure 1(c). Once aligned, CT scans were re-sliced according to the same orientation as the MRI scan. The muscle belly in the sagittal-oblique plane was identified as the most lateral slice where the scapular spine comes into contact with the scapular body (Y-view, shown in Figure 2). The cross-sectional area of each rotator cuff muscle at the Y-view was then measured on both MRI and CT scans.

Muscle morphology assessment

After validating the accuracy of CT scans for measures of muscle size using the data from ten patients, MA and FI for all patients were assessed using the original CT scans. Thresholding was applied as needed to enhance the clarity of the muscles on CT scans.

Muscle atrophy

The total muscle size was determined by measuring the total cross-sectional area of each rotator cuff muscle at the Y-view using manual segmentation techniques, as previously described.[17,22–24] During segmentation, the assessor (author DS) was blinded to the participant's glenoid characteristics and grouping. Fat-free muscle area within the segmented muscle boundary was also segmented and measured. Fat-free muscle was identified using its specific Hounsfield unit (HU) ranges of −29 HU to +150 HU.[25] The ratio of the combined infraspinatus and teres minor

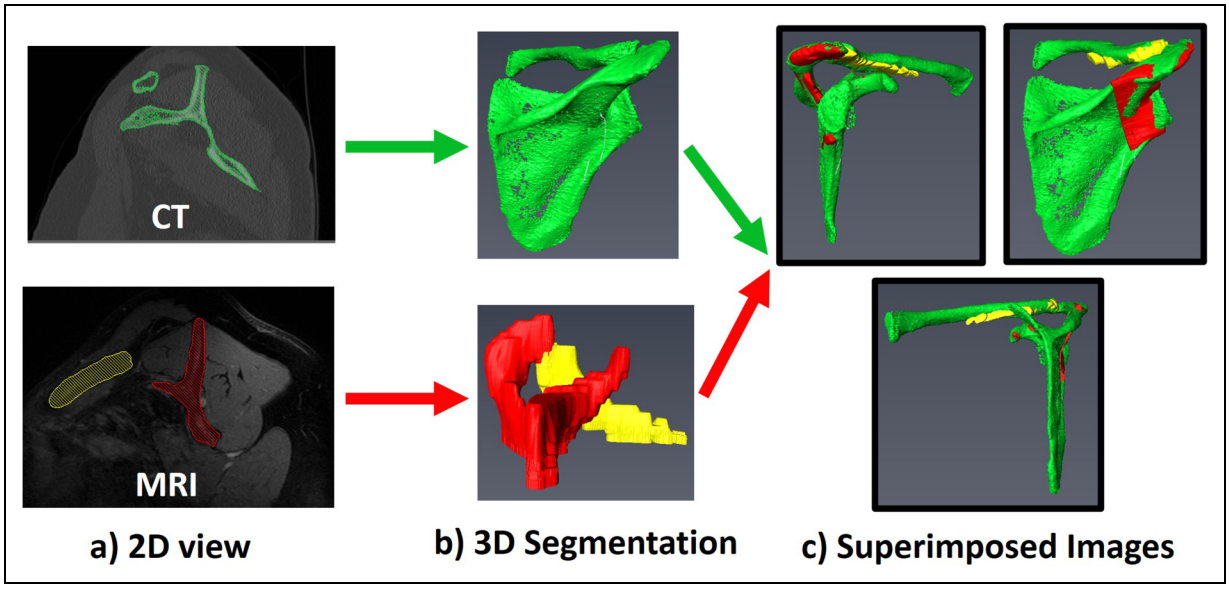

Figure 1. (a) The scapula from MRI and CT was segmented on 2-dimensional (2D) slices. (b) Three-dimensional (3D) images of the scapula were obtained from the 2D segmentations. (c) The 3D image of the scapula obtained from the CT segmentation was then re-oriented to superimpose it with the 3D image obtained from the MRI segmentation.

areas to subscapularis area was calculated for both the total muscle area and fat-free muscle area due to its implications for force balance across the glenohumeral joint in the axial plane.[13,14]

Fatty infiltration

As previously described by Lapner et al.[6] (2015), fat-free muscle and FI areas within each segmented muscle boundary at a single image slice (the Y-view) were quantified using defined Hounsfield units (HU) for the CT scans (Figure 2). FI and fat-free muscle were distinguished from each other using the HU ranges of −190 HU to −30 HU and −29 HU to +150 HU, respectively.[25] Percent FI for each rotator cuff muscle was calculated by dividing the FI area by the sum of FI and fat-free muscle areas.

Glenoid morphology assessment

Glenoid inclination and version were measured with pre-operative radiographs and CT scans. Glenoid inclination angle (β angle) was measured according to Maurer et al.[26] (2012), and the glenoid version (α or Friedman angle) was measured according to Friedman et al.[27] (1992). Inclination and version were measured on the pre-operative Grashey and axial radiographs, respectively. Similar methods were followed to measure the α and β angles on CT images at approximately the mid-glenoid level. Glenoid morphology was assessed on both radiographs and representative CT images and classified as per Walch et al.[28,29] (1998 and 1999) and Bercik et al.[30] (2016) into A1, A2, B1, B2, B3, and D types. All classifications were made by two shoulder and elbow fellowship trained orthopedic surgeons (authors GU and AA). Any discrepancies were discussed between the two surgeons to reach consensus.

Statistical analysis

For each rotator cuff muscle, a paired t-test was performed to compare the cross-sectional area measurements between MRI and CT scans to characterize the accuracy of CT scans for measures of muscle size. Pearson correlation coefficients were calculated to evaluate the agreement of the measurements from MRI and CT scans. Any value greater than 0.90 was considered a very high correlation.[31] Separate regression analyses were performed to characterize the association of glenoid version and inclination with rotator cuff muscle MA (i.e., total cross-sectional area, fat-free muscle area, and the ratio of infraspinatus and teres minor muscle areas to subscapularis muscle area) and FI. Additional two-sample t-tests were performed to determine the differences in MA and FI across: 1) A glenoids versus B glenoids; and 2) A glenoids versus non-A glenoids. Data for individual Walch glenoid types (A1, A2, B1, B2, and B3) was assessed for normality using the Shapiro–Wilk test. As the majority of the data was non-parametric, differences in MA and FI across individual Walch glenoid types (A1, A2, B1, B2, and B3) were separately evaluated using a Kruskal–Wallis test for each MA and FI variable. Multiple pairwise comparisons were performed using Dunn's procedure. Groups were also evaluated for differences in sex, age, and body mass index (BMI) to determine if further analyses were needed to account for these differences. Specifically, chi-squared

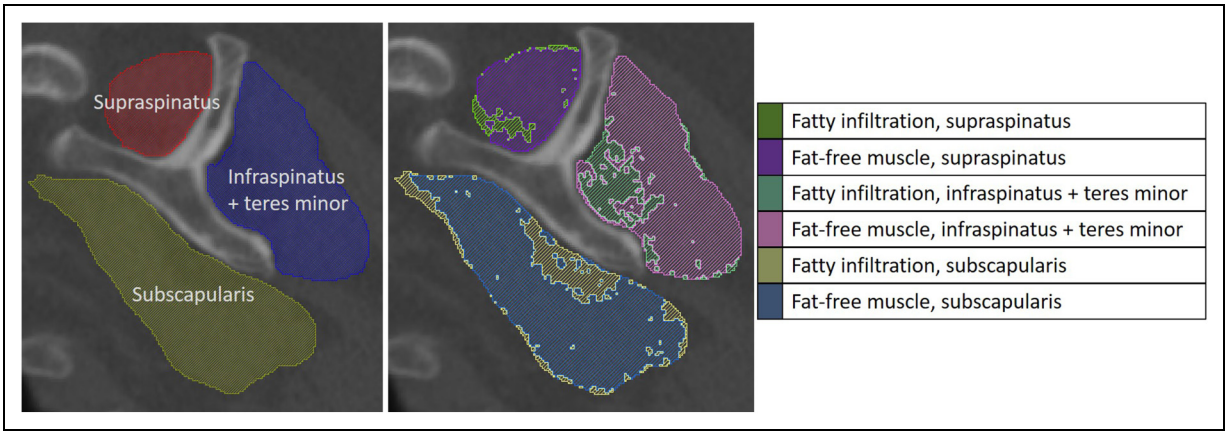

Figure 2. Rotator cuff muscles were segmented, and the FI and fat-free muscle within the segmented muscle boundary were identified according to their Hounsfield unit ranges.

tests were performed to detect any differences in sex distribution among glenoid groups (A versus B, A versus non-A, and individual Walch glenoid types). Two-sample t-tests were performed to detect any differences in age and BMI between: 1) A glenoids versus B glenoids, and 2) A glenoids versus non-A glenoids. ANOVA was used to detect differences in age and BMI among individual Walch glenoid types. Analyses were performed using XLSTAT in Microsoft Excel (Microsoft Corp., Redman, WA), with significance set at $p < 0.05$.

Results

Patient population

A total of 66 patients were evaluated. One patient was excluded from the study because their CT scan was of insufficient quality from which to obtain quantitative measurements. An additional four patients were excluded from any analysis because three did not include the entire cross-section of the infraspinatus and teres minor muscles, and one patient had a lipoma that compressed these muscles. One more patient was excluded from any analysis as their CT scan did not include the entire cross-section of the muscle. After these exclusions, 61 patients (61 shoulders) were evaluated. There was only one D glenoid, so it was not included in the Kruskal–Wallis analysis.

Among the 61 patients, 37 of them were female (60%). The cohort age was 64.2 ± 10.3 years, and BMI was 32.4 ± 5.9 kg/m^2. There were no differences in sex, age, and BMI across Walch glenoid types (Table 1).

Validation of CT scans for measures of muscle size

There were ten patients within the cohort with both preoperative CT and MRI scans. No differences were detected in mean cross-sectional area measurements between CT and MRI scans, with very high correlations observed between the measurements from the two scans ($p = 0.797$, $R = 0.998$ for supraspinatus; $p = 0.386$, $R = 0.944$ for infraspinatus and teres minor; and $p = 0.639$, $R = 0.993$ for subscapularis; Table 2). The mean total muscle area, fat-free muscle area, and percent FI for each rotator cuff muscle, as well as the mean inclination and version measures from the entire study cohort are listed in Table 3.

Muscle atrophy

The total muscle area and fat-free muscle area were not associated with glenoid inclination or version (Table 4). The ratio of infraspinatus and teres minor muscles to subscapularis muscle was not associated with glenoid inclination or version, for both the total muscle area and fat-free muscle area (Table 4). Compared to Walch type A glenoids, Walch type B glenoids ($p = 0.030$) and non-A glenoids ($p = 0.041$) had larger infraspinatus and teres minor total muscle area (Table 5). Individual Walch glenoid type analyses demonstrated that Walch type B2 glenoids had larger infraspinatus and teres minor total muscle area relative to A2 glenoids ($p = 0.012$, Figure 3(b)). There were no differences in fat-free muscle area of individual rotator cuff muscles between Walch type A versus B glenoids, or between Walch type A versus non-A glenoids (Table 5). Similarly, no differences in fat-free muscle areas were observed across individual Walch glenoid types (Figure 3(d) to (f)). No differences in the ratio of infraspinatus and teres minor to subscapularis were observed between Walch type A versus B glenoids or between Walch type A versus non-A glenoids, for both the total muscle area and fat-free muscle area (Table 5). However, individual Walch glenoid type analyses demonstrated that Walch type B2 glenoids had larger ratios of infraspinatus and teres minor total muscle area to subscapularis total muscle area relative to A1 glenoids ($p = 0.026$)

Table 1. Differences in sex, age, and BMI across Walch glenoid types based on chi-squared tests (for sex), two-sample t-tests (for age and BMI; between A versus B and A versus non-A), and ANOVA (for age and BMI; across individual Walch glenoid types).

	Sex, *n* (percent)			
Glenoid types ($n=61$)	Female	Male	Age, mean (SD), years	BMI, mean (SD), kg/m^2
A ($n=20$)	13 (65.0)	7 (35.0)	63.4 (9.2)	32.6 (5.4)
B ($n=40$)	23 (57.5)	17 (42.5)	64.3 (10.9)	32.0 (6.0)
non-A (B + D, $n=41$)	24 (58.5)	17 (41.5)	64.6 (10.9)	32.2 (6.1)
p-value (A vs B)	0.58		0.72	0.69
p-value (A vs non-A)	0.63		0.64	0.80
Glenoid subtypes				
A1 ($n=11$)	7 (63.6)	4 (36.4)	63.3 (10.1)	33.3 (6.4)
A2 ($n=9$)	6 (66.7)	3 (33.3)	63.4 (8.6)	31.8 (4.1)
B1 ($n=10$)	6 (60.0)	4 (40.0)	66.7 (12.6)	31.4 (6.9)
B2 ($n=17$)	9 (52.9)	8 (47.1)	62.8 (7.1)	32.5 (4.9)
B3 ($n=13$)	8 (61.5)	5 (38.5)	64.4 (13.9)	31.8 (7.0)
p-value	0.96		0.91	0.9
D ($n=1$)	1	0	77	41.4

SD, standard deviation.
*Statistically significant at $p < 0.05$.

Table 2. Comparison of muscle area measurements from MRI and CT scans.

	Total muscle area, mean (SD), cm^2			
	MRI	CT	*t*-test, *p*-value	Pearson correlation coefficient, *R*
Supraspinatus ($n=10$)	4.71 (1.26)	4.70 (1.26)	0.797	0.998**
Infraspinatus and teres minor ($n=10$)	11.92 (2.68)	11.65 (2.83)	0.386	0.944**
Subscapularis ($n=10$)	12.54 (3.44)	12.47 (3.55)	0.639	0.993**

SD: standard deviation.
*Statistically significant at $p < 0.05$.
**Very high correlation.

and A2 glenoids ($p=0.038$, Figure 3(g)). There were no differences in the ratio of infraspinatus and teres minor fat-free muscle area to subscapularis fat-free muscle area among Walch glenoid types (Table 5; Figure 3(h)).

Fatty infiltration

FI was not associated with glenoid inclination or version (Table 4). No differences in supraspinatus FI were observed between Walch type A and non-A glenoids or between Walch type A and B glenoids (Table 5). Based on the multiple pairwise comparisons, Walch type B3 glenoids had greater supraspinatus FI relative to A2 glenoids ($p=0.032$, Figure 4(a)). There were no differences in infraspinatus and teres minor FI between Walch type A versus B glenoids or between Walch type A versus non-A glenoids (Table 5). Walch type B3 glenoids had greater infraspinatus and teres minor FI compared to A1 glenoids ($p=0.039$),

Table 3. Mean total muscle area, fat-free muscle area, and percent fatty infiltration for each rotator cuff muscle, and mean glenoid inclination and version.

Measures of muscle morphology	Mean (SD)
Supraspinatus ($n = 61$)	
Total muscle area (cm^2)	5.35 (1.30)
Fat-free muscle area (cm^2)	2.46 (1.06)
Fatty infiltration (percent)	35.9 (11.5)
Infraspinatus and teres minor ($n = 61$)	
Total muscle area (cm^2)	15.60 (4.12)
Fat-free muscle area (cm^2)	7.38 (3.44)
Fatty infiltration (percent)	33.7 (12.2)
Subscapularis ($n = 61$)	
Total muscle area (cm^2)	17.68 (4.59)
Fat-free muscle area (cm^2)	8.77 (4.28)
Fatty infiltration (percent)	31.7 (13.1)
Infraspinatus and teres minor to subscapularis ratio ($n = 61$)	
Total muscle area ratio	0.90 (0.16)
Fat-free muscle area ratio	0.87 (0.18)
Measures of glenoid morphology	Mean (SD)
Inclination (degrees, $n = 61$)	79.9 (15.8)
Version (degrees, $n = 61$)	11.5 (9.2)

SD: standard deviation.
All measurements were performed from CT scans.

Table 4. Correlations between rotator cuff muscle atrophy, fatty infiltration, and glenoid inclination and version.

	Inclination		Version	
Supraspinatus ($n = 61$)	*R*	*p*-value	*R*	*p*-value
Total muscle area (cm^2)	0.179	0.168	0.229	0.075
Fat-free muscle area (cm^2)	0.205	0.114	0.053	0.687
Fatty infiltration (percent)	0.113	0.385	0.121	0.352
Infraspinatus and teres minor ($n = 61$)				
Total muscle area (cm^2)	0.054	0.682	0.079	0.543
Fat-free muscle area (cm^2)	0.095	0.466	0.036	0.784
Fatty infiltration (percent)	0.072	0.582	0.102	0.433
Subscapularis ($n = 61$)				
Total muscle area (cm^2)	0.029	0.0825	0.039	0.768
Fat-free muscle area (cm^2)	0.159	0.222	0.013	0.919
Fatty infiltration (percent)	0.157	0.228	0.047	0.718
Infraspinatus and teres minor to subscapularis ratio ($n = 61$)				
Total muscle area ratio	0.148	0.254	0.164	0.206
Fat-free muscle area ratio	0.046	0.724	0.027	0.837

R: Pearson correlation coefficient.
*Statistically significant at $p < 0.05$.

A2 glenoids ($p = 0.028$), and B1 glenoids ($p = 0.038$, Figure 4(b)). No differences in subscapularis FI were detected between Walch type A versus B glenoids, or between Walch type A versus non-A glenoids (Table 5). Walch type B3 glenoids had larger subscapularis FI relative to A2 glenoids ($p = 0.032$, Figure 4(c)).

Discussion

The role of rotator cuff muscle atrophy and fatty infiltration as it relates to glenoid morphology in primary glenohumeral osteoarthritis is not fully understood. Thus, the main purpose of this study was to explore the associations of rotator cuff muscle FI and MA and the classification of glenoid morphology. Our study revealed that B3 glenoids had greater FI of all rotator cuff muscles, and B2 glenoids had larger relative size of infraspinatus and teres minor muscles compared to the subscapularis. Although this study cannot comment on the causal role of FI and MA in glenoid wear, our findings support an association between FI, MA, and glenoid morphology. In addition, this study showed that muscle size measurements from CT have very high correlation with MRI.

Contrary to Arenas-Miquelez[16] (2021) and Moverman et al.[13] (2022), but in agreement with Donohue et al.[12] (2018), we found that Walch type B3 glenoids had higher percent FI across all rotator cuff muscles. This finding could suggest that the weakening of the rotator cuff muscles could change the force distribution across the glenohumeral joint, leading to the eccentric glenoid wear seen in Walch type B3 glenoids. However, it is also possible that eccentric glenoid wearing and development of FI are two parallel, but separate, processes that occur as glenohumeral osteoarthritis progresses.

These results have potential clinical implications for a surgeon when making surgical treatment decisions for patients with B3 glenoids. There are typically two treatment

Table 5. Differences in rotator cuff fatty infiltration, total muscle area, fat-free muscle area, and infraspinatus and teres minor to subscapularis ratio across Walch glenoid types based on *t*-tests and Kruskal–Wallis tests.

	Fatty infiltration, mean (SD), percent			Total muscle area, mean (SD), cm^2			Fat-free muscle area, mean (SD), cm^2			Infraspinatus and teres minor to subscapularis ratio, mean (SD)	
Glenoid types	Supraspinatus	Infraspinatus and Teres minor	Subscapularis	Supraspinatus	Infraspinatus and Teres minor	Subscapularis	Supraspinatus	Infraspinatus and Teres minor	Subscapularis	Total muscle area ratio	Fat-free muscle area ratio
A ($n=20$)	33.1 (12.4)	30.7 (12.9)	27.8 (13.8)	5.17 (1.34)	14.23 (3.10)	17.64 (4.47)	2.64 (1.06)	7.84 (4.23)	9.55 (4.41)	0.84 (0.19)	0.82 (0.14)
B ($n=40$)	37.4 (11.0)	35.6 (11.5)	33.8 (12.5)	5.46 (1.29)	16.42 (4.38)	17.82 (4.70)	2.35 (1.07)	7.11 (3.04)	8.34 (4.26)	0.93 (0.15)	0.89 (0.19)
non-A (B + D, $n=41$)	37.3 (10.9)	35.1 (11.7)	33.5 (12.5)	5.44 (1.29)	16.28 (4.42)	17.70 (4.71)	2.37 (1.06)	7.16 (3.02)	8.39 (4.21)	0.93 (0.14)	0.89 (0.19)
p-value (A vs B)	0.20	0.16	0.11	0.43	0.030*	0.89	0.33	0.50	0.32	0.062	0.13
p-value (A vs non-A)	0.21	0.21	0.13	0.47	0.041*	0.96	0.36	0.52	0.33	0.069	0.13
Glenoid subtypes											
A1 ($n=11$)	34.3 (12.4)	31.1 (13.1)	29.8 (13.3)	5.21 (0.77)	15.49 (2.97)	19.21 (3.31)	2.64 (1.15)	8.40 (5.27)	10.42 (5.39)	0.82 (0.13)	0.80 (0.14)
A2 ($n=9$)	31.6 (12.9)	30.2 (13.3)	25.5 (14.7)	5.13 (1.88)	12.68 (2.61)	15.73 (5.13)	2.63 (1.01)	7.16 (2.60)	8.47 (2.74)	0.57 (0.25)	0.85 (0.15)
B1 ($n=10$)	33.8 (12.4)	31.6 (11.9)	29.0 (14.4)	5.06 (1.13)	15.67 (3.51)	17.47 (3.91)	2.76 (1.57)	8.43 (4.09)	10.25 (6.15)	0.90 (0.11)	0.86 (0.20)
B2 ($n=17$)	36.9 (12.3)	34.8 (12.4)	34.5 (12.2)	5.63 (1.49)	17.10 (4.56)	18.12 (5.27)	2.27 (0.85)	7.08 (2.17)	7.91 (2.60)	0.96 (0.16)	0.93 (0.21)
B3 ($n=13$)	40.8 (7.3)	49.7 (9.1)	36.7 (11.1)	5.56 (1.17)	16.10 (4.93)	17.70 (4.81)	2.14 (0.85)	6.15 (2.98)	7.43 (4.16)	0.91 (0.15)	0.86 (0.18)
p-value	0.16	0.12	0.14	0.88	0.17	0.68	0.75	0.53	0.47	0.13	0.49
D ($n=1$)	32.1	15.6	20.5	4.49	10.67	12.96	3.00	8.90	10.29	0.82	0.87

SD: standard deviation.
*Statistically significant at $p < 0.05$.

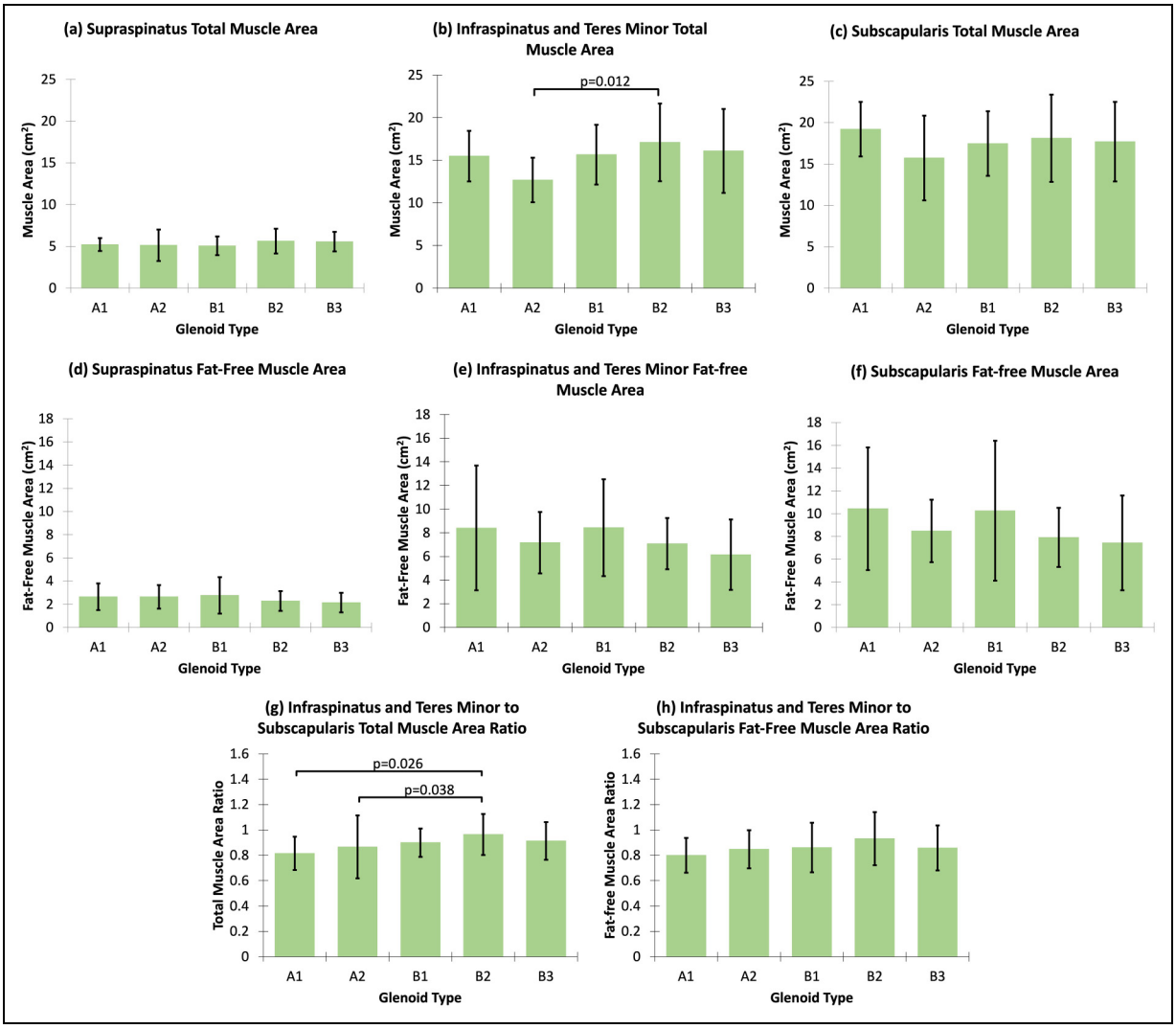

Figure 3. Multiple pairwise comparisons for the differences in rotator cuff muscle atrophy across Walch glenoid subtypes. Only statistically significant p-values are included.

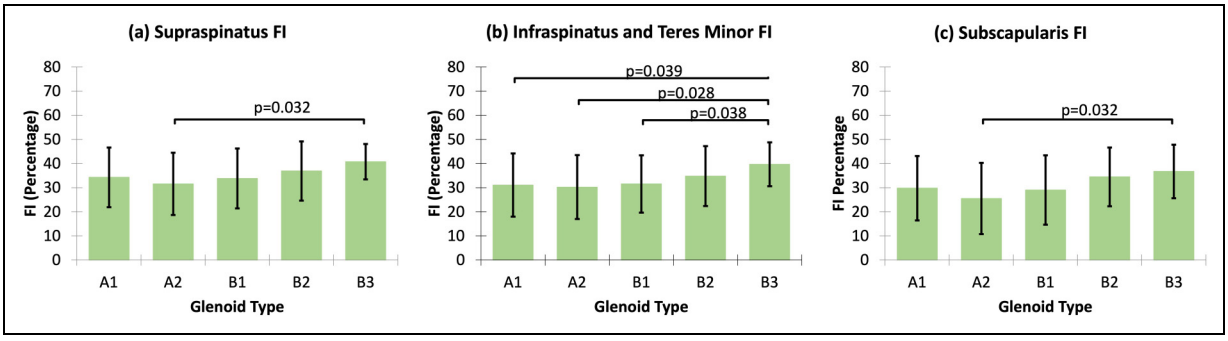

Figure 4. Multiple pairwise comparisons for the differences in rotator cuff FI across Walch glenoid subtypes. Only statistically significant *p*-values are included. FI: fatty infiltration.

options for patients with B3 gleniods; (1) Anatomic total shoulder arthroplasty with or without an augmented glenoid to accommodate the bone deformity or (2) Reverse total shoulder arthroplasty. Based on these results, further consideration for a reverse total shoulder arthroplasty may be considered in the setting of a B3

glenoid since this implant does not rely as heavily on the integrity of the rotator cuff. The weaker rotator cuff muscles due to increased FI in B3 glenoids could potentially lead to poorer long-term results using an anatomic reconstruction. However, the authors advise caution, as further investigation is warranted to determine the differences in outcomes of these treatment options for patients with B3 glenoids, if any exists.

Consistent with previous work,[12,13] our study did not find any associations between rotator cuff muscle FI and glenoid inclination. Donohue et al.[12] (2018) and Moverman et al.[13] (2022) both reported a link between higher-grade infraspinatus and teres minor muscle FI and greater glenoid version. We did not find a correlation between glenoid version and percent FI for any of the rotator cuff muscles. It is possible that the small sample size ($n = 61$ in our study versus $n = 190$ and $n = 127$ in prior studies[12,13]) prevented detection of a significant correlation, which was seen in prior studies. Furthermore, Donohue et al.[12] (2018) and Moverman et al.[13] (2022) assessed FI using the semi-quantitative Goutallier classification system, which is prone to high inter- and intra-observer variability.[17–19] Thus, in the current study, we quantitatively determined FI based on the characteristic HU ranges for fat and muscle.

To our knowledge, this is the first study to quantify fat-free muscle to investigate its association with glenoid morphology, which provides a more direct assessment of the contribution of muscle fibers. While prior studies focused on the total muscle area,[13–15] less attention has been given to fat-free muscle area, which is the force-generating component of the total area and impacts the force balance at the joint. Contrary to our hypothesis, we did not find an association between the fat-free muscle area and glenoid deformity. It appears that the total muscle size and FI are the potentially contributing factors in the development of glenoid deformity rather than the fat-free muscle area.

Walch type B glenoids had larger total infraspinatus and teres minor muscle area relative to type A glenoids. However, we did not find any differences in the relative size of infraspinatus and teres minor compared to subscapularis between Walch type A glenoids versus B glenoids. Our findings are in agreement with the study by Moverman et al.[13] (2022), which reported larger infraspinatus and teres minor muscle size in Walch type B glenoids relative to type A glenoids, with no differences in the relative size of infraspinatus and teres minor muscles compared to the subscapularis between these two groups. In contrast, Chalmers et al.[15] (2020) reported increased infraspinatus and teres minor muscle volume compared to the subscapularis muscle volume in Walch type B glenoids. They hypothesized that the asymmetric atrophy of subscapularis relative to infraspinatus and teres minor results in a net force directed posteriorly across the joint, contributing to the development of the eccentric glenoid wear seen in Walch type B glenoids. Recently, O'Neill et al.[32] (2021) demonstrated that Walch type B glenoids with greater retroversion had larger posterior deltoid area, suggesting a similar force imbalance. Considering our results in the setting of the findings of O'Neill et al.[32] (2021), it is likely that there are other factors in addition to the infraspinatus and teres minor and subscapularis muscles, such as the deltoid muscle, that could contribute to any force imbalance across the glenohumeral joint and development of eccentric glenoid wear. The contributions from other muscles may explain why we did not find any differences in the ratio of infraspinatus and teres minor to subscapularis muscle size between Walch type A and type B glenoids in the current study, without discounting the hypothesis that the force imbalance plays a role in the development of eccentric glenoid wear. Further studies are needed to identify which muscles and other soft tissues may contribute to this force imbalance. Although we did not find any differences in the relative size of infraspinatus and teres minor compared to subscapularis between Walch type A and type B glenoids, when comparing each subtype against each other, type B2 glenoids had larger relative infraspinatus and teres minor areas compared to the subscapularis area than types A1 and A2 glenoids. This is consistent with the findings of Aleem et al.[14] and supports the potential role of the force imbalance between posterior and anterior rotator cuff muscles in the development of glenoid deformity.

The strengths of our study included the quantification of fat-free muscle to further understand the association of MA and consequent force imbalance with eccentric glenoid wear. We also quantified FI using predefined HU of fat instead of the semi-quantitative Goutallier classification used in previous studies, which is a method known to be limited by its high inter- and intra-observer variability.[17–19] However, there were several limitations to our study. First, due to cost and availability, CT scans were only acquired for patients with complex glenoid morphology, limiting our sample size to 66 shoulders. Furthermore, our sample did not include enough Walch type C ($n = 0$) and D ($n = 1$) glenoids to be able to include these presentations in our statistical analyses. Future work should examine how the associations observed here extend to Walch type C and D glenoids. Only ten patients had both pre-operative CT and MRI scans; thus, we had a small sample size to characterize the correlation for muscle size between CT and MRI scans. Moreover, we measured MA and FI at a single slice from CT scans, and although this method is consistent with previous literature, 3D volume analyses may be needed to further confirm our results. This study was limited to TSA candidates with primary glenohumeral osteoarthritis. Further studies are needed in healthy patients and patients with less advanced arthritic joints for comparison to a control group. Also, this was a retrospective study with measurements taken at a single,

pre-operative time point; thus, it was not possible to establish a causal role of rotator cuff MA and FI in the progression of glenoid wear. However, we uncovered associations between the muscle and glenoid morphology. Future studies should perform a temporal analysis of shoulder images to determine any causal relationships. More work is also needed to study whether muscle strengthening rehabilitation exercises can prevent the progression of arthritic glenoid wear or improve TSA outcomes by offsetting the imbalance of forces at the glenohumeral joint.

Conclusions

In this study, Walch type B3 glenoids had greater fatty infiltration of all rotator cuff muscles, and Walch type B2 glenoids had larger relative size of infraspinatus and teres minor muscles compared to the subscapularis. More work is needed to identify other muscles and soft tissues that could contribute to the imbalance of forces at the glenohumeral joint that drive eccentric glenoid wear. Additional studies are needed to determine if there is a causal role of rotator cuff muscle atrophy and fatty infiltration in the progression of glenoid wear.

Contributorship

DS was involved in the literature review, data collection and analysis, funding acquisition, study design, and validation of results. PP was involved in gaining ethical approval, data curation, ethical approval and data collection. GL was involved in the study design. GU was involved in the data curation, data collection, and project administration. AA was involved in the formulation of research goals, data curation, study design, project administration, patient recruitment, and supervision of the study. MV was involved in the formulation of research goals, data collection and analysis, funding acquisition, study design, validation of results, project administration, and supervision of the study. DS wrote the first draft of the manuscript. All authors reviewed and edited the manuscript and approved the final version of the manuscript.

Declaration of conflicting interest

The authors declared the following potential conflicts of interest with respect to the research, authorship, and/or publication of this article: GU is a consultant for Stryker, DePuy Synthes, Globus, and Aevumed which is unrelated to this work. AA is a consultant for and has received royalties from Zimmer Biomet and Aevumed which is unrelated to the subject of this work.

Ethical approval

Ethical approval for this study was obtained from the Institutional Review Board at the Penn State College of Medicine (study number: 00011438).

Funding

The authors disclosed receipt of the following financial support for the research, authorship, and/or publication of this article: Research reported in this publication was supported by the National Center for Advancing Translational Sciences, NIH Grants TL1 TR002016 and UL1 TR002014. The content is solely the responsibility of the authors and does not necessarily represent the official views of the NIH.

Informed consent

Informed consent was not sought for the present study because it is a retrospective study where all data is extracted from pre-existing patient medical records.

Guarantor

MV

ORCID iD

Deniz Siso https://orcid.org/0000-0001-9277-7375

References

1. Kuzel BR, Grindel S, Papandrea R, et al. Fatty infiltration and rotator cuff atrophy. *J Am Acad Orthop Surg* 2013; 21: 613–623.
2. Lippitt ST and Matsen FR. Mechanisms of glenohumeral joint stability. *Clin Orthop Relat Res* 1993; 291: 20–28.
3. Lippitt SB, Vanderhooft JE, Harris SL, et al. Glenohumeral stability from concavity-compression: a quantitative analysis. *J Shoulder Elbow Surg* 1993; 2: 27–35.
4. Magarey ME and Jones MA. Specific evaluation of the function of force couples relevant for stabilization of the glenohumeral joint. *Man Ther* 2003; 8: 247–253.
5. Vidt ME, Santago II AC, Marsh AP, et al. Modeling a rotator cuff tear: individualized shoulder muscle forces influence glenohumeral joint contact force predictions. *Clin Biomech (Bristol, Avon)* 2018; 60: 20–29.
6. Lapner PL, Jiang L, Zhang T, et al. Rotator cuff fatty infiltration and atrophy are associated with functional outcomes in anatomic shoulder arthroplasty. *Clin Orthop Relat Res* 2015; 473: 674–682.
7. Sayed-Noor AS, Pollock R, Elhassan BT, et al. Fatty infiltration and muscle atrophy of the rotator cuff in stemless total shoulder arthroplasty: a prospective cohort study. *J Shoulder Elbow Surg* 2018; 27: 976–982.
8. Chan K, Knowles NK, Chaoui J, et al. Characterization of the Walch B3 glenoid in primary osteoarthritis. *J Shoulder Elbow Surg* 2017; 26: 909–914.
9. Habermeyer P, Magosch P, Luz V, et al. Three-dimensional glenoid deformity in patients with osteoarthritis: a radiographic analysis. *J Bone Joint Surg Am* 2006; 88: 1301–1307.
10. Walch G, Moraga C, Young A, et al. Results of anatomic nonconstrained prosthesis in primary osteoarthritis with biconcave glenoid. *J Shoulder Elbow Surg* 2012; 21: 1526–1533.
11. Young AA, Walch G, Pape G, et al. Secondary rotator cuff dysfunction following total shoulder arthroplasty for primary glenohumeral osteoarthritis: results of a multicenter study with more than five years of follow-up. *J Bone Joint Surg Am* 2012; 94: 685–693.
12. Donohue KW, Ricchetti ET, Ho JC, et al. The association between rotator cuff muscle fatty infiltration and glenoid morphology in glenohumeral osteoarthritis. *J Bone Joint Surg Am* 2018; 100: 381–387.

13. Moverman MA, Puzzitiello RN, Menendez ME, et al. Rotator cuff fatty infiltration and muscle atrophy: relation to glenoid deformity in primary glenohumeral osteoarthritis. *J Shoulder Elbow Surg* 2022; 31: 286–293.
14. Aleem AW, Chalmers PN, Bechtold D, et al. Association between rotator cuff muscle size and glenoid deformity in primary glenohumeral osteoarthritis. *J Bone Joint Surg Am* 2019; 101: 1912–1920.
15. Chalmers PN, Beck L, Miller M, et al. Glenoid version associates with asymmetric rotator cuff muscle atrophy in those with Walch B-type glenohumeral osteoarthritis. *J Am Acad Orthop Surg* 2020; 28: 547–555.
16. Arenas-Miquelez A, Liu VK, Cavanagh J, et al. Does the Walch type B shoulder have a transverse force couple imbalance? A volumetric analysis of segmented rotator cuff muscles in osteoarthritic shoulders. *J Shoulder Elbow Surg* 2021; 30: 2344–2354.
17. Chalmers PN, Beck L, Stertz I, et al. Do magnetic resonance imaging and computed tomography provide equivalent measures of rotator cuff muscle size in glenohumeral osteoarthritis? *J Shoulder Elbow Surg* 2018; 27: 1877–1883.
18. Khazzam M, Kuhn JE, Mulligan E, et al. Magnetic resonance imaging identification of rotator cuff retears after repair: interobserver and intraobserver agreement. *Am J Sports Med* 2012; 40: 1722–1727.
19. Lippe J, Spang JT, Leger RR, et al. Inter-rater agreement of the Goutallier, Patte, and Warner classification scores using preoperative magnetic resonance imaging in patients with rotator cuff tears. *Arthroscopy* 2012; 28: 154–159.
20. Lehtinen J, Tingart M, Apreleva M, et al. Practical assessment of rotator cuff muscle volumes using shoulder MRI. *Acta Orthop Scand* 2003; 74: 722–729.
21. Tingart MJ, Apreleva M, Lehtinen JT, et al. Magnetic resonance imaging in quantitative analysis of rotator cuff muscle volume. *Clin Orthop Relat Res* 2003; 415: 104–110.
22. Holzbaur KR, Murray WM and Delp SL. A model of the upper extremity for simulating musculoskeletal surgery and analyzing neuromuscular control. *Ann Biomed Eng* 2005; 33: 829–840.
23. Vidt ME, Daly M, Miller ME, et al. Characterizing upper limb muscle volume and strength in older adults: a comparison with young adults. *J Biomech* 2012; 45: 334–341.
24. Vidt ME, Santago II AC, Tuohy CJ, et al. Assessments of fatty infiltration and muscle atrophy from a single magnetic resonance image slice are not predictive of 3-dimensional measurements. *Arthroscopy* 2016; 32: 128–139.
25. Aubrey J, Esfandiari N, Baracos VE, et al. Measurement of skeletal muscle radiation attenuation and basis of its biological variation. *Acta Physiol (Oxf)* 2014; 210: 489–497.
26. Maurer A, Fucentese SF, Pfirrmann CW, et al. Assessment of glenoid inclination on routine clinical radiographs and computed tomography examinations of the shoulder. *J Shoulder Elbow Surg* 2012; 21: 1096–1103.
27. Friedman RJ, Hawthorne KB and Genez BM. The use of computerized tomography in the measurement of glenoid version. *J Bone Joint Surg Am* 1992; 74: 1032–1037.
28. Walch G, Badet R, Boulahia A, et al. Morphologic study of the glenoid in primary glenohumeral osteoarthritis. *J Arthroplasty* 1999; 14: 756–760.
29. Walch G, Boulahia A, Boileau P, et al. Primary glenohumeral osteoarthritis: clinical and radiographic classification. The Aequalis group. *Acta Orthop Belg* 1998; 64: 46–52.
30. Bercik MJ, Kruse II K, Yalizis M, et al. A modification to the Walch classification of the glenoid in primary glenohumeral osteoarthritis using three-dimensional imaging. *J Shoulder Elbow Surg* 2016; 25: 1601–1606.
31. Hinkle DE, Wiersma W and Jurs SG. *Applied statistics for the behavioral sciences*. 5th ed. Boston: Houghton Mifflin, 2003.
32. O'Neill DC, Christensen GV, Hillyard B, et al. Glenoid version associates with deltoid muscle asymmetry in Walch B-type glenohumeral osteoarthritis. *JSES Int* 2021; 5: 282–287.